AlN Passivation Layer-Mediated Improvement in Tensile Failure of Flexible ZnO:Al Thin Films

Hong Rak Choi,[†] Bhaskar Chandra Mohanty,[†] Jong Seong Kim,[‡] and Yong Soo Cho*[,†]

Department of Materials Science and Engineering, Yonsei University, Seoul 120-749, Korea, LCD R&D Center, Samsung Electronics Co., Gyeonggi-Do 446-711, Korea

ABSTRACT AlN passivation layer-mediated improvement in tensile failure of ZnO:Al thin films on polyethersulfone substrates is investigated. ZnO:Al films without any passivation layer were brittle with a crack-initiating bending strain ε_c of only about 1.13% with a saturated crack density ρ_s of 0.10 μm^{-1} and a fracture energy Γ of 49.6 J m^{-2}. On passivation by an AlN overlayer, the fracture energy of the system increased considerably and a corresponding improvement in ε_c was observed. AlN layers deposited at higher discharge powers yielded higher fracture energy and exhibited better performance in terms of ε_c and ρ_s.

KEYWORDS: flexible electronics • AlN passivation • ZnO thin films • crack density • fracture energy

INTRODUCTION

In recent years, ZnO-based thin films have been extensively studied because of their potential in a variety of applications such as flat panel displays, touch-screen devices, solar cells, etc. (1). Fostered by the increasing popularity of flexible electronics, there are significant efforts to grow these films on flexible substrates, for example, on 200 μm thick metal or plastic sheets, which can provide flexibility and portability (2, 3). Being transparent, the plastic substrates are more advantageous, especially in flexible display applications that utilize curved surfaces. The films grown on these plastic substrates, however, are brittle and can withstand only limited strain that may arise due to various mechanical stresses caused by bending, stretching, etc. (4−7). Thus, structural integrity and stability of films on the flexible substrates become major issues in designing devices. Hence, there are increasing endeavors to predict the onset of the failure and, subsequently, to provide solutions to overcome the reliability problem.

Recently, Ni et al. have studied cracking behavior of 1 μm thick ZnO:Al thin films in face-in and face-out bending tests (8). The results suggest that multiple cracks in ZnO:Al appear in the films when the tensile strain increases by more than 1.38 and 0.50% in face-in and face-out configurations, respectively, which puts a serious constraint in flexible display designs. Considering the huge potential of ZnO:Al thin films in flexible electronics, it is thus of interest to devote research efforts to increase the resistance of the films against mechanical strains. In recent years, in thin film technology, especially in the integrated circuit industry, passivation layers have shown significant effects on performance of the devices. It is the objective of the present work to verify whether such a passivation layer can help improving mechanical resistance of ZnO:Al thin films grown on a plastic substrate. In this work, we have chosen high-thermal-conduction AlN as a passivation layer for improvement in tensile failure of the ZnO:Al thin films grown on polyethersulfone (PES) substrates. Besides its chemical stability, high thermal conductivity, wide band gap, extreme hardness, and high melting temperature, the choice of AlN films stems from recent meaningful success in the use of AlN as a passivation layer in the heterojunction field effect transistors and other electronic devices (9, 10).

EXPERIMENTAL SECTION

The detailed procedure of the ZnO:Al film deposition is given in our previous work (11). The distance between the centers of target and substrate was kept at 7 cm. During the deposition, the substrates were rotated at 8 rpm about their axes. PES substrates with the dimension of 20 mm × 20 mm in area and 200 μm in thickness were used. The ZnO:Al film of ~200 nm thickness was sputter-deposited at a constant rf power of 150 W in pure Ar ambient (~2 mtorr) at room temperature. The AlN thin films (~200 nm) were grown by reactive rf magnetron sputtering on ZnO:Al-coated PES substrates held at 75 °C at various powers. The base pressure was less than 1×10^{-6} Torr and the working pressure during the deposition was fixed at 2 mtorr by allowing an argon−nitrogen gas mixture (Ar:N_2 = 3:1) through mass-flow controllers. Adhesion between the films and with the substrate was examined by a typical peel test, which revealed a strong bonding between the interfaces. Structural properties were investigated by X-ray diffraction (XRD) using a PANalytical model X'Pert PRO XRD unit using Cu−K_α radiation in Bragg-Brentano ($\theta/2\theta$) geometry. Analysis of the XRD patterns of the ZnO:Al thin films revealed the formation of the well-crystallized hexagonal wurtzite single phase with prominent *c*-axis orientation. On the other hand, the AlN thin films were found to be amorphous at 150 and 200 W. Peak traces corresponding to hexagonal AlN phase were observed only for the films deposited at 250 W. All films (both ZnO:Al and AlN) showed excellent UV−visible transmittance (~85%). The sur-

* To whom correspondence should be addressed. E-mail: ycho@yonsei.ac.kr.
Received for review May 2, 2010 and accepted August 9, 2010
[†] Yonsei University.
[‡] Samsung Electronics Co.
DOI: 10.1021/am100386s
2010 American Chemical Society

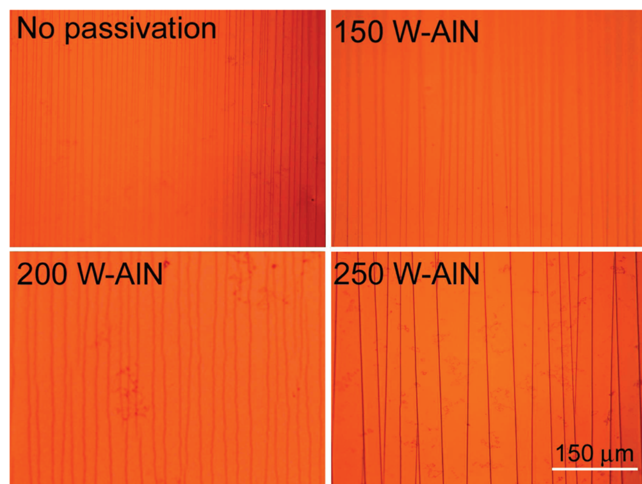

FIGURE 1. Optical micrographs indicating multiple straight cracks in the unpassiviated and passivated ZnO:Al thin films on PES substrates at bending strain of ∼3%. The bending direction is perpendicular to the crack lines.

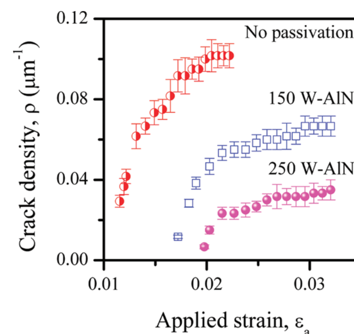

FIGURE 2. Plot of crack density of unpassiviated and AlN-passivated ZnO:Al thin films as a function of applied bending strain.

face microstructure and roughness of samples before the fracture studies were investigated by atomic force microscopy (AFM, Digital Instruments, Nanoscope IIId), carried out in air at room temperature in tapping mode of operation using Al-backcoated Si cantilevers. The surface of the AlN film prepared at 250W was based on densely packed crystallites having an average size of ∼20 nm and the root-mean-square roughness of only ∼2.5 nm.

The bending evaluation method used in this study to measure the flexibility and crack initiation is similar to that used in earlier studies (7, 8). The sample was loaded between two parallel holders and was gradually bent into a sinusoidal shape, thus exposing films to a tensile stress, under an applied force provided by a micrometer. The cracking behavior that resulted from the center of the sample by the bending test was recorded in situ by an optical microscope and expressed in terms of the number of cracks generated. Although the quantitative stress level and stress distribution are not available, we believe that there exists a certain stress distribution over the specimen upon bending. This is evident from the different distribution of cracks depending on the sample position. For instance, the bending region around the center (that has a higher applied tensile stress) tends to bring a higher number of cracks (8).

Since the Young's modulus of the ZnO:Al films ($E_f = 150$ GPa) (12) is much larger than that for the PES substrates ($E_s = 2.6$ GPa) (13), the neutral surface in the structure is shifted upward toward the film, and the applied strain ε_a at top of the film is approximately calculated as (8, 14)

$$\varepsilon_a = \left(\frac{t_f + t_s}{2r}\right)\frac{(1 + 2\eta + \chi\eta^2)}{(1 + \eta)(1 + \chi\eta)} \qquad (1)$$

where t_f and t_s are thickness of the film and the substrate, respectively, $\eta = t_f/t_s$, $\chi = E_f/E_s$, and r is the radius of the curvature of the center of the bent sample. The values of r were calculated using the formula given elsewhere (7). Because the thicknesses of ZnO:Al and the AlN films are nearly same, the Young's modulus for the bilayer was calculated using the moduli of the ZnO:Al (150 GPa) and AlN (300 GPa) based on the rule of mixtures.

RESULTS AND DISCUSSION

Figures 1 and 2 show the examples of crack development on the film surface and the relation of crack density to the applied strain, respectively. The in situ optical microscopy of the bending test revealed that beyond a critical value of applied strain, sporadic cracks perpendicular to the tensile stress direction were generated in the ZnO:Al films. The number of the parallel cracks increased and the average spacing between the cracks was reduced dramatically with increase in applied strain ε_a. However, with further increase in strain, the crack density ρ and the crack spacing λ remained nearly constant indicating a saturated state. The examples in Figure 1 compare the unpassivated and AlN-passivated ZnO:Al thin films subjected to the same saturated strain of ∼3.0%, demonstrating clear effects of passivation as well as different powers on the cracking behavior. Increasing power from 150 to 250 W resulted in the decrease in the number of cracks and the increase of spacing between cracks for the identical applied strain.

The critical strain ε_c, which corresponds to the minimum applied strain required to initiate cracks in the films, was determined by extrapolating the corresponding ρ versus ε_a curve to $\rho = 0$ in the plots of Figure 2. We find that for our ZnO:Al/PES structures the values of critical strain ε_c, saturated crack density ρ_s and saturated crack spacing λ_s are about 1.13%, 0.10 μm^{-1} and 10 μm, respectively. It is noted that the saturated crack spacing λ_s is nearly inverse of the saturated crack density ρ_s, which agrees well with the reported studies (15, 16). When the ZnO:Al films were passivated by an AlN overlayer, significant improvement in the bending failure of the films was observed. The increase in critical strain by more than 70% and the substantial decrease in the saturated crack density were observed for the 250W films with respect to the unpassivated film. The extracted parameters ε_a and ρ_s are plotted as a function of rf power in Figure 3. This figure also contains the fracture energy data of the corresponding films.

The fracture energy Γ for the ZnO:Al films and the AlN/ZnO:Al bilayers were calculated using the energy criterion proposed earlier for the multiple film cracking phenomenon (6, 15). As the crack length is several times larger than the film thickness, the cracks propagate steadily. Further, it is assumed that the cracks extend through the entire film and not into the substrate. Conventionally, the cracks in the films can occur if the change in the strain energy due to such breaking of the film is in equilibrium with the energy

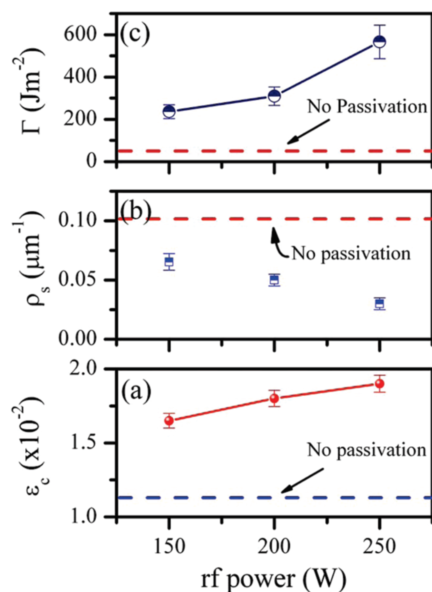

FIGURE 3. Plot of (a) critical strain ε_c, (b) saturated crack density ρ_s, and (c) fracture energy Γ of the AlN/ZnO:Al/PES structures as functions of rf-power used to grow the AlN layer. In each panel, the value corresponding to ZnO:Al/PES structure (i.e., without passivation layer) is shown as the dashed line.

required for film cracking. In the absence of a mismatch strain, the fracture energy Γ is given as (6, 15)

$$\Gamma = \frac{3}{4\alpha}\frac{E_f\varepsilon_c^2(1 - 2\nu_f\nu_s + \nu_s^2)}{(1 - \nu_f^2)} \qquad (2)$$

when $\alpha = [(3)/(2\beta(1 + \nu_s))((1)/(\beta) + ((1 - \nu_f^2)E_s)/((1 - \nu_s\nu_f)E_f))]^{1/2}(1)/(t_f)$, ν_s and ν_f are Poisson's ratio of the substrate and the film, respectively, and β is the thickness ratio of the effective substrate to the film. It is important to note the calculation of Γ involves the effective substrate thickness, rather than the actual substrate thickness. Hence, β must be estimated first.

Hsueh and Wereszczak have shown that the relation between the applied strain and the crack density can be given by (15)

$$\frac{\varepsilon_a}{\varepsilon_c} = \sqrt{\frac{3}{2f}}$$

where

$$f = 4\tanh\left(\frac{\alpha l}{2}\right) - \frac{e^{\alpha l} - e^{-\alpha l} + 2\alpha l}{e^{\alpha l} + e^{-\alpha l} + 2} - 2\tanh(\alpha l) + \frac{1}{2}\frac{e^{2\alpha l} - e^{-2\alpha l} + 4\alpha l}{e^{2\alpha l} + e^{-2\alpha l} + 2} \qquad (3)$$

In eq 3, l relates to the crack density ρ through the relation $l = 2/3\rho$ (17). In Figure 4, the computed and the experimental curves for the function f versus the applied strain ε_a are plotted for the unpassivated and the AlN passivated ZnO:Al

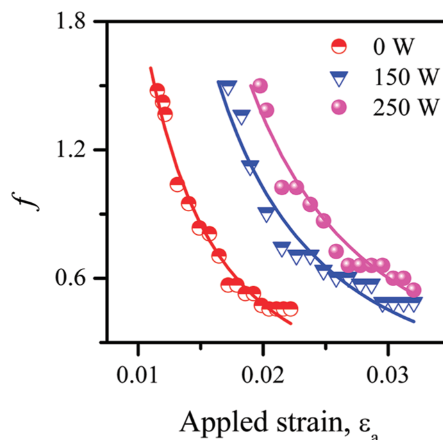

FIGURE 4. Computed (sold lines) and experimental (symbols) curves of the function f (defined in eq 3 in the text) of the unpassiviated and AlN-passivated ZnO:Al thin films as a function of applied bending strain.

Table 1. Results Obtained by the Analysis of Cracking Behavior of Only AlN Thin Films on PES Substrates

rf power (W)	ε_c (× 10^{-2})	ρ_s (μm^{-1})	β	Γ (× 10^3 J m^{-2})
150	1.40 ± 0.04	0.08 ± 0.01	30.2 ± 0.5	0.23 ± 0.03
200	2.40 ± 0.07	0.06 ± 0.01	32.7 ± 0.3	0.74 ± 0.09
250	3.00 ± 0.09	0.03 ± 0.01	42.3 ± 0.3	1.46 ± 0.17

thin films. The calculated values agree well with the experimental curves when $\beta = 16.8$ is assumed for the unpassivated ZnO:Al film. The corresponding values for the film passivated by the AlN layer grown with 150, 200, and 250 W are 12.7, 14.1, and 24.3, respectively. Using these values the fracture energy is calculated to be ~236.1, 309.6, and 565.9 J m^{-2} for the corresponding passivated layers in contrast to 49.6 J m^{-2} obtained for the unpassivated layer. The lower fracture energy of the unprotected film indicates relatively more brittle nature of the films. It is obvious that the passivation of the ZnO:Al thin films by an equivalent thickness AlN layer improves the tensile failure, mainly by enhancing the fracture energy. We have separately calculated the fracture energy of only the AlN films (of similar thickness) grown on PES substrates. The results obtained from the analysis are listed in Table 1. The only AlN films have higher fracture energies at high powers than the AlN/ZnO:Al bilayers. Further, the fracture energies exhibit a near-linear dependence on the discharge power employed to grow only the AlN thin films directly on the PES substrate. The power dependence of the fracture energy in both cases of AlN/ZnO and only AlN thin films may be associated with the degree of the constraining effect on crack propagation driven by microstructural features (18). In the case of sputter deposition of thin films, a higher discharge power provides the depositing species with higher energy, thus higher atomic mobility on the growing surfaces. This eventually leads to a well-adherent film with a dense microstructure (higher packing density of crystallites) characterized by uniform grains and low intrinsic defects such as pin-holes, cracks, etc. (19). Such a film is believed to be less susceptible to tensile failures.

CONCLUSIONS

In summary, we have investigated fracture behavior of sputter-deposited thin ZnO:Al films on PES substrates. The films exhibited a crack-initiating bending strain of only about 1.13% with a saturated crack density of 0.10 μm^{-1}. However, passivation by an equivalent thickness AlN layer significantly improved the tensile failure of the films, apparently by increasing the fracture energy. The ZnO:Al films passivated by an AlN layer grown at 250 W showed a critical strain of ~1.90% (nearly 70% improvement in comparison to the unpassivated films). Higher rf power is believed to yield better adherent films with a dense microstructure and low intrinsic defects, which is less-susceptible to tensile failures. As obtained by the separate experiment, higher fracture energies of only AlN films at high powers support well the effectiveness of the AlN thin films as a passivation layer.

Acknowledgment. This research was supported by Basic Science Research Program through the National Research Foundation of Korea (NRF) funded by the Ministry of Education, Science and Technology (2009-0077678). One of the authors (B.C.M.) gratefully acknowledges the financial support from the Ministry of Education, Government of Korea, in the form of a BK 21 fellowship.

REFERENCES AND NOTES

(1) Gregory, P. C. In *Flexible Flat Panel Displays*; David, C. P., Hyo-Young, Y., Burag, Y., Eds.; John Wiley and Sons: Chichester, U.K., 2005; p 79.
(2) Kim, D.; Ahn, J.; Choi, W. M.; Kim, H.; Kim, T.; Song, J.; Huang, Y. Y.; Liu, Z.; Lu, C.; Rogers, J. A. *Science* **2008**, *320*, 507.
(3) Someya, T.; Kato, Y.; Sekitani, T.; Iba, S.; Noguchi, Y.; Murase, Y.; Kawaguchi, H.; Sakurai, T. *Proc. Natl. Acad. Sci. U.S.A.* **2005**, *102*, 12321.
(4) Heinrich, M.; Gruber, P.; Orso, S.; Handge, U. A.; Spolenak, R. *Nano Lett.* **2006**, *6*, 2027.
(5) Leterrier, Y.; Wyser, Y.; Månson, J. A. E.; Hilborn, J. *J. Adhes.* **1994**, *44*, 213.
(6) Hsueh, C. H.; Yanaka, M. *J. Mater. Sci.* **2003**, *38*, 1809.
(7) Park, S.; Ahn, J.; Feng, X.; Wang, S.; Huang, Y.; John, A. R. *Adv. Funct. Mater.* **2008**, *18*, 2673.
(8) Ni, J. L.; Zhu, X. F.; Pei, Z. L.; Gong, J.; Sun, C.; Zhang, G. P. *J. Phys. D: Appl. Phys.* **2009**, *42*, 175404.
(9) Chen, D. J.; Tao, Y. Q.; Chen, C.; Zhang, R.; Zheng, Y. D.; Wang, M. J.; Shen, B.; Li, Z. H.; Jiao, G.; Chen, T. S. *Appl. Phys. Lett.* **2006**, *89*, 252104.
(10) Fan, Z. Y.; Li, J.; Nakarmi, M. L.; Lin, J. Y.; Jiang, H. X. *Appl. Phys. Lett.* **2006**, *88*, 073513.
(11) Mohanty, B. C.; Jo, Y. H.; Yeon, D. H.; Choi, I. J.; Cho, Y. S. *Appl. Phys. Lett.* **2009**, *95*, 062103.
(12) Navamathavan, R.; Kim, K.; Hwang, D.; Park, S.; Hahn, J.; Lee, T. G.; Kim, G. *Appl. Surf. Sci.* **2006**, *253*, 464.
(13) http://i-components.co.kr/kor/product/product04_2.asp.
(14) Suo, Z.; Ma, E. Y.; Gleskova, H.; Wagner, S. *Appl. Phys. Lett.* **1999**, *74*, 1177.
(15) Hsueh, C. H.; Wereszczak, A. A. *J. Appl. Phys.* **2004**, *96*, 3501.
(16) Miller, D. C.; Foster, R. R.; Zhang, Y.; Jen, S. H.; Bertrand, J. A.; Lu, Z.; Seghete, D.; O'Patchen, J. L.; Yang, R.; Lee, Y. C.; George, S. M.; Dunn, M. L. *J. Appl. Phys.* **2009**, *105*, 093527.
(17) Yanaka, M.; Miyamoto, T.; Tsukahara, Y.; Takeda, N. *Compos. Interfaces* **1999**, *6*, 409.
(18) Niu, R. M.; Liu, G.; Wang, C.; Zhang, G.; Ding, X. D.; Sun, J. *Appl. Phys. Lett.* **2007**, *90*, 161907.
(19) Cheng, H.; Hing, P. *Surf. Coat. Technol.* **2003**, *167*, 297.

AM100386S